THE JOURNAL OF BIOLOGICAL CHEMISTRY VOL. 289, NO. 23, pp. 16085–16099, June 6, 2014

TMTC1 and TMTC2 Are Novel Endoplasmic Reticulum Tetratricopeptide Repeat-containing Adapter Proteins Involved in Calcium Homeostasis*[S]

Received for publication, January 28, 2014, and in revised form, April 2, 2014 Published, JBC Papers in Press, April 24, 2014, DOI 10.1074/jbc.M114.554071

Johan C. Sunryd[‡§1], Banyoon Cheon[§¶], Jill B. Graham[‡§], Kristina M. Giorda[‡§], Rafael A. Fissore[§¶], and Daniel N. Hebert[‡§2]

From the Departments of [‡]Biochemistry and Molecular Biology and [¶]Veterinary and Animal Sciences, [§]Program in Molecular and Cellular Biology, University of Massachusetts, Amherst, Massachusetts 01003

Background: The ER is organized into subdomains containing large protein complexes that help to perform a variety of functions.
Results: TMTC1 and TMTC2 are ER membrane proteins with large TPR-containing adapter domains that mediate associations with SERCA2B.
Conclusion: TMTC1 and TMTC2 are ER adapter proteins that influence intracellular calcium levels.
Significance: TMTC1 and TMTC2 are regulators of calcium homeostasis.

The endoplasmic reticulum (ER) is organized in part by adapter proteins that nucleate the formation of large protein complexes. Tetratricopeptide repeats (TPR) are well studied protein structural motifs that support intermolecular protein-protein interactions. TMTC1 and TMTC2 were identified by an *in silico* search as TPR-containing proteins possessing N-terminal ER targeting signal sequences and multiple hydrophobic segments, suggestive of polytopic membrane proteins that are targeted to the secretory pathway. A variety of cell biological and biochemical assays was employed to demonstrate that TMTC1 and TMTC2 are both ER resident integral membrane proteins with multiple clusters of TPR domains oriented within the ER lumen. Proteomic analysis followed by co-immunoprecipitation verification found that both proteins associated with the ER calcium uptake pump SERCA2B, and TMTC2 also bound to the carbohydrate-binding chaperone calnexin. Live cell calcium measurements revealed that overexpression of either TMTC1 or TMTC2 caused a reduction of calcium released from the ER following stimulation, whereas the knockdown of TMTC1 or TMTC2 increased the stimulated calcium released. Together, these results implicate TMTC1 and TMTC2 as ER proteins involved in ER calcium homeostasis.

The endoplasmic reticulum (ER)[3] is an organelle composed of a continuous membrane envelope and lumen that is compartmentalized into numerous functional regions (1). The organization of the ER is directed in part by extrinsic factors that organize the rough ER (ribosomes) and the contiguous nuclear envelope (lamina and lamina receptors), as well as through interactions with the cytoskeleton (microtubules), organelles (Golgi and mitochondria), or the plasma membrane (2). ER resident adapter proteins that nucleate the formation of large protein complexes also support the compartmentalization of the ER (3–5). The organization of the ER contributes to its ability to efficiently perform functions in the maturation, quality control, and trafficking of secretory pathway cargo, calcium regulation, and lipid synthesis (6–8). These activities contribute to the maintenance of general cellular homeostasis; however, many questions still remain as to how the organization of the ER is maintained.

Tetratricopeptide repeats (TPR) are protein structural motifs that support protein-protein interactions. A single TPR domain consists of a degenerate 34-amino acid sequence that is composed of two anti-parallel helices (9, 10). A minimum of three consecutive TPR domains is required to form a functional unit, and this is the most common number of TPR found in a cluster (9). Clusters composed of up to 16 sequential TPR have been observed. Proteins with three TPR domains in a cluster favor the recognition of short and defined sequences, whereas proteins with long stretches of consecutive TPR domains tend to be more promiscuous in their selectivity. For example, the Hsp70-Hsp90 organizing protein (HOP) uses two separate clusters of three consecutive TPR domains to bind the EEVD sequence located at the C termini of Hsp70 and Hsp90, facilitating the handoff of a substrate from one chaperone to another (11, 12). In contrast, the *O*-linked *N*-acetylglucosamine transferase possesses 12 consecutive TPR domains that are proposed to bind and prepare substrates for modification (13). Tom70 displays a combination of TPR clusters as it uses a cluster of three TPR domains to recognize the C terminus of Hsp70 for substrate delivery and a second cluster of seven TPR domains to potentially prepare substrates for mitochondrial import (14).

* This work was supported, in whole or in part, by National Institutes of Health Grants GM086874 (to D. N. H.) and HD051872 (to R. A. F.) from USPHS.
[S] This article contains supplemental Table S1.
[1] Supported in part by National Institutes of Health Training Grant GM008515.
[2] To whom correspondence should be addressed: Dept. of Biochemistry and Molecular Biology, University of Massachusetts, 240 Thatcher Road Amherst, MA 01003. Tel.: 413-545-0079; Fax: 413-545-3291; E-mail: dhebert@biochem.umass.edu.
[3] The abbreviations used are: ER, endoplasmic reticulum; BiP, binding immunoglobulin protein; C, cytosol; DNJ, *N*-butyl deoxynojirimycin; Endo H, endoglycosidase H; N, nucleus; P, pellet; PNGase F, peptide-*N*-glycosidase F; qRT-PCR, quantitative RT-PCR; S, supernatant; TPR, tetratricopeptide repeat.

These diverse cellular functions are coordinated by TPR domains and their ability to bind to a range of ligands.

SEL1L and $p58^{IPK}$ (also called ERdj6) are the only ER TPR-containing proteins that have been characterized in mammalian cells. SEL1L nucleates a large ER membrane complex involved in ER-associated degradation (4). $p58^{IPK}$ is an ER co-chaperone that interacts with BiP to facilitate protein folding (15, 16). Given the extensive utilization of TPR domains in metazoans to support protein-protein interactions, the ER is expected to contain additional TPR domain proteins that contribute to complex formation and ER organization.

An *in silico* approach was used to expand our understanding of ER adapters that participate in the organization of the ER using TPR domains. TMTC1 and TMTC2 were identified as TPR-containing proteins that possess potential N-terminal ER targeting sequences and multimembrane spanning regions. They were both found to reside in the ER membrane with their TPR domains oriented within the ER lumen. A role for TMTC1 and TMTC2 as adapter proteins was supported by their appearance in large molecular weight complexes. A shotgun proteomics approach was employed that identified SERCA2B as a potential binding partner for TMTC1 and TMTC2, as well as calnexin for TMTC2. Manipulation of the expression levels of TMTC1 and TMTC2 combined with live cell calcium measurements demonstrated that TMTC1 and TMTC2 influenced calcium sequestering in the ER. Collectively, these findings showed that TMTC1 and TMTC2 are two novel TPR-containing ER adapters involved in calcium homeostasis.

EXPERIMENTAL PROCEDURES

Reagents and Plasmids—Dulbecco's modified Eagle's medium (DMEM), calcium-free DMEM, fetal calf serum, penicillin, streptomycin, and Zysorbin were purchased from Invitrogen. 1-Deoxynojirimycin (DNJ) and Easy-Tag [^{35}S]Cys/Met were purchased from Toronto Research Chemicals and PerkinElmer Life Sciences, respectively. S-protein-agarose beads and S tag antibody were purchased from EMD Millipore. Endo H, PNGase F, avian myeloblastosis virus first strand synthesis kit, and all cloning reagents were purchased from New England Biolabs. FastStart SYBR Green qPCR mix was purchased from Roche Diagnostics, and all primers were acquired from IDT DNA. Anti-mouse HRP IgG, anti-rabbit HRP IgG, and protein A-Sepharose CL-4B were purchased from GE Healthcare. Antibodies directed toward the following antigens were also purchased: SERCA2 (Cell Signaling); Myc (Cell Signaling); calnexin (Enzo Life Sciences); calreticulin (Thermo Scientific); and GM130 (BD Biosciences). TMTC1 and TMTC2 cDNA were purchased (Open Biosystems) and cloned into a pcDNA3.1 A−, a plasmid harboring either a C-terminal S or Myc tag, using standard molecular biology techniques. TMTC1 and TMTC2 were tagged with GFP by inserting the GFP cDNA between the coding region and the C-terminal S tag. These constructs were termed $TMTC1^{GFP}$ and $TMTC2^{GFP}$. The pcDNA3.1 A− S tag backbone was modified to possess an N-terminal BiP signal sequence prior to the multiple cloning site and a KDEL sequence after the C-terminal S tag. The TPR domains of TMTC1 and TMTC2 were cloned into this plasmid to create $TMTC1^{TPR}$ and $TMTC2^{TPR}$ constructs. shRNA plasmids were purchased from Qiagen. All other chemicals were obtained from Sigma.

In Silico Analysis of TMTC1 and TMTC2—The primary amino acid sequence of TMTC1 and TMTC2 was analyzed by UniProtKB and TPRpred to identify the number and position of putative TPR domains (17, 18). Hydrophobic domains were identified by the ΔG software, which predicts transmembrane domains (19). Homologues of TMTC1 and TMTC2 were identified by Basic Local Alignment Search Tool searches (20). The similarity and identify of TMTC1 and TMTC2 were determined using Clustal Omega software (21).

Tissue Culture—Human embryonic kidney (HEK) 293T or COS7 cells were grown in DMEM supplemented with 10% fetal calf serum, 100 units/ml penicillin, and 100 mg/ml streptomycin and incubated at 37 °C in 5% CO_2. Cells were transfected with polyethyleneimine and the appropriate plasmids for 16 h.

Microscopy—Cells were fixed with 4% paraformaldehyde in phosphate-buffered saline (PBS) for 10 min at room temperature followed by permeabilization with methanol for 10 min at −20 °C. Slides were stained with the indicated primary antibody followed by staining with the appropriate Alexa Fluor 488 or 594 secondary antibodies in immunostaining buffer (20 mM HEPES (pH 7.5), 150 mM NaCl, 2 mM $MgCl_2$, 1 mM EGTA, and 2% bovine serum albumin). Slides were rinsed and mounted onto coverslips with VectaShield (Vector Laboratories). Images were obtained with a Fluoview 1000 MPE, IX81 motorized inverted research microscope (Olympus Inc.) equipped with a Hamamatsu C8484-05G camera. All images were acquired with a Plan Apo N ×60 1.42NA lens and processed by using the FV10-ASW and the Adobe Photoshop software.

Radiolabeling, Affinity Purification, and Glycosylation Assay—Radiolabeling of proteins with [^{35}S]Cys/Met was performed as described previously (22). Cells were lysed in MNT buffer (0.5% Triton X-100, 20 mM MES, 100 mM NaCl, 20 mM Tris-HCl (pH 7.5)). All steps were conducted at 4 °C. The postnuclear supernatant was isolated by centrifugation followed by preclearing with Zysorbin for 1 h. Cleared supernatant was incubated with S-protein-agarose beads overnight and subsequently washed twice with MNT buffer. After the final MNT wash, glycosylation assays were performed by adding appropriate buffers and either mock, Endo H, or PNGase F enzymes according to the manufacturer's protocol. Finally, reducing sample buffer was added to all samples, and they were analyzed by SDS-PAGE.

Alkaline Extraction—Alkaline extraction was performed as described previously (23). Briefly, radiolabeled cells were resuspended in ice-cold homogenization buffer (20 mM HEPES (pH 7.5), 5 mM KCl, 120 mM NaCl, 1 mM EDTA, and 0.3 M sucrose) and passed through a 22-gauge needle 20 times. All subsequent steps were conducted at 4 °C. The homogenate was centrifuged at 1,000 × *g* for 10 min to pellet the nuclear fraction. The remaining postnuclear supernatant was centrifuged at 45,000 rpm in Beckman rotor (TLA 120.2) for 10 min to separate the cytosol (supernatant) from the cellular membranes (pellet). The cellular membrane fraction was resuspended in homogenization buffer, and a portion of the resuspended membranes was incubated with 0.1 M Na_2CO_3 (pH 11.5) for 30 min on ice. The alkaline-extracted portion was centrifuged at 65,000 rpm for 20 min through a sucrose cushion (50 mM triethanolamine,

0.3 M sucrose (pH 7.5)) to separate soluble proteins from membrane proteins in the supernatant and pellet, respectively. The pH was adjusted in the alkaline-extracted sample with 1 M Tris-HCl (pH 7.5). An excess of MNT was added to all fractions, and immunoprecipitation or affinity precipitation was performed with protein A-Sepharose and appropriate antisera or with S-protein-agarose, respectively.

Trypsin Protection—Radiolabeled cells were homogenized, and the microsomes were purified as described above. Microsomes were resuspended in homogenization buffer, and 10 μg of trypsin and/or Triton X-100 was added to a final concentration of 0.1%. After incubation for 15 min at 27 °C, the reaction was quenched with 5 μg of soybean trypsin inhibitor. Samples were then resuspended in MNT, and affinity purification was performed as described above.

qRT-PCR—HEK293T cells were treated with either 5 mM dithiothreitol, 0.5 μM thapsigargin, 5 μg/ml tunicamycin, or starved for Cys and Met for 8 h prior to RNA isolation with the RNeasy mini kit (Qiagen). One μg of purified RNA was reverse-transcribed into cDNA using the avian myeloblastosis virus reverse transcriptase kit (New England Biolabs). qRT-PCRs were performed in 20-μl reactions using FastStart universal SYBR Green master (Rox) kit (Roche Diagnostics Corp.) on an Mx3000P real time PCR machine (Agilent Technologies) according to the manufacturer's instructions. Changes in mRNA levels were calculated using the change in cycle threshold value method with β-actin as the reference gene (24). Statistical analysis of the data was calculated using GraphPad Prism 4.0 (GraphPad Software), and the significance between treatment groups was determined using one-way analysis of variance followed by Tukey's multiple comparison tests.

The following primers were used: *β-actin* (5′-GCACTCTTCCAGCCTTCC-3′ and 5′-TGTCCACGTCACACTTCATG-3′), *BiP* (5′-GCTGTTTCTATTGGCCTTTCTC-3′ and 5′-TGTCTCTTTCACCAGCATCG-3′), *TMTC1* (5′-GCTGTTTCTATTGGCCTTTCTC-3′ and 5′-TGTCTCTTTCACCAGCATCG-3′), *TMTC2* (5′-GATGTCTTTGTCTTTCACAGGC-3′ and 5′-TGTTTCCCATCCAGTATAACCG 3′).

shRNA Knockdown—Polycistronic plasmids that express a cytoplasmic GFP and a predesigned shRNA were purchased from Qiagen. HEK293T cells were transfected with the shRNA for 24 h prior to RNA purification and qRT-PCR as described above. To determine transfection efficiency, HEK293T cells were transfected for 24 h followed by trypsinization and resuspension in DMEM. Resuspended cells were loaded onto a Guava easy flow Cytometer (Millipore). Transfected *versus* nontransfected cells were distinguished based on fluorescence from the cytoplasmic GFP. A total of 5,000 events were counted per measurement.

In-gel Digestion and LC-MS/MS—Transfected cells were homogenized, and microsomes were purified as described above. Microsomes were resuspended in mass spectrometry buffer (50 mM HEPES (pH 7.4), 300 mM NaCl, 25 mM EDTA, 1% Triton X-100) followed by affinity purification with S-protein-agarose beads. Beads were washed twice in MS buffer and twice with 50 mM ammonium bicarbonate followed by resuspension in reducing sample buffer. Samples were loaded onto an SDS-PAGE and allowed to run ~1 cm into a gel before trypsin digestion. Tryptic peptides were lyophilized, resuspended, and loaded onto a custom column that eluted into a Proxeon Easy nanoLC system directly coupled to an LTQ Orbitrap Velos mass spectrometer (Thermo Scientific). The Orbitrap was set to achieve full scans from 350 to 2000 m/z with a resolution of 6000. The LTQ ion trap instrument performed 10 scans. Data were analyzed with either Mascot Distiller (Matrix Science, Inc.) or Extract_MSN (Thermo Scientific). The Mascot Search engine (Matrix Science, Inc.) and SwissProt database were used for protein identification. Trypsin digestion and subsequent steps were performed by the Proteomics and Mass Spectrometry Facility, University of Massachusetts Medical School for mass spectrometric analysis.

Immunoblotting and Affinity Purification—Transfected cells were suspended in homogenization buffer. Part of the homogenate was centrifuged at 45,000 rpm for 10 min to purify microsomes; the pellet was resuspended in reducing sample buffer and was considered the total membrane fraction. An excess of MNT buffer was added to an equal portion of homogenate, and preclearing was performed with control agarose beads, followed by affinity purification with S-protein-agarose beads overnight. Beads were washed twice in MNT buffer. Reducing sample buffer was added, and samples were loaded onto SDS-PAGE. Proteins were transferred to a polyvinylidene difluoride membrane and immunoblotted with the appropriate antisera. Blots were developed, and TIFF files were acquired using a G:Box (New England BioGroup), and densitometric quantification of Western blots were performed using MultiGauge software (Fujifilm). The TMTC2 and calnexin interaction was calculated by dividing the amount of calnexin in the S tag affinity purification with the amount of calnexin in the total membrane fraction, with or without DNJ. The interaction with TMTC2 and calnexin in the absence of DNJ was then set to 100%. Error bars represent the standard deviation for three independent experiments.

Sucrose Gradient Centrifugation—Transfected cells were lysed in MNT, and the postnuclear supernatant was layered on top of a continuous 10–40% sucrose gradient with a 60% cushion in MNT buffer. The gradients were centrifuged for 16 h at 4 °C with a Beckman SW41 at 145,000 × g. Standards used to determine sedimentation velocities were bovine serum albumin (4.6 S, 66 kDa), β-amylase (8.9 S, 200 kDa), and bovine thyroglobulin (19 S, 669 kDa). After centrifugation, 9% of the total gradient volume was collected per fraction, and proteins were isolated with trichloroacetic acid precipitation. Samples were resuspended in reducing sample buffer and analyzed by immunoblotting with the appropriate antisera. After the last fraction was collected, the pellet was processed by adding sample buffer directly to the ultracentrifugation tube.

Live Cell Calcium Measurement—HEK293T cells were plated on a glass bottom 3.5-cm dish and transfected the following day. Cells were loaded with 2.5 μM Fura2 acetoxymethyl ester (Molecular Probes, Eugene, OR) and 2.5 μM Pluronic F-127 for 45 min 16 h post-transfection. Plates were washed with fresh media and incubated for 45 min to allow hydrolysis of the Fura2 acetoxymethyl ester. Plates were then rinsed with fresh media and placed on an inverted microscope with a ×20 objective (Nikon Corp., Tokyo, Japan). Fluorescence was measured every 20 s, and the excitation wavelength was switched

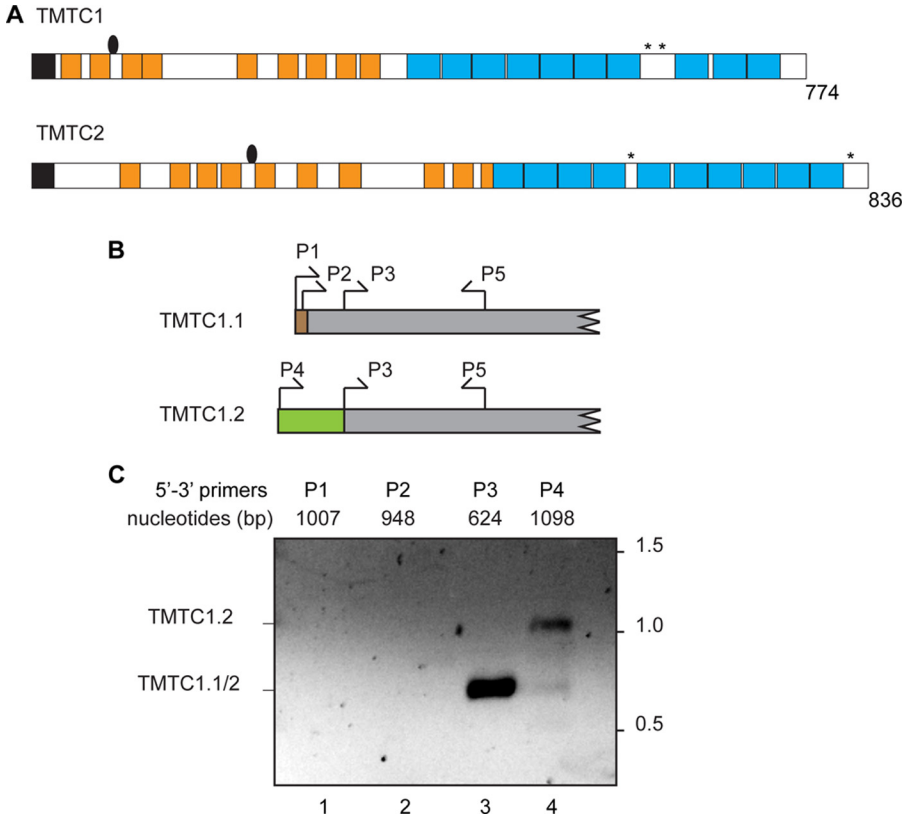

FIGURE 1. **Organization and transcription of TMTC1 and TMTC2 isoforms.** *A*, organization of TMTC1 (TMTC1 isoform 2) and TMTC2 with signal sequences (*black boxes*), hydrophobic domains (*orange boxes*), and TPR domains (*blue boxes*) as designated. Endogenous and introduced *N*-linked glycosylation sites are indicated by *black ovals* and *asterisks*, respectively. *B*, there are two possible isoforms of TMTC1 designated as TMTC1.1 (TMTC1 isoform 1 (NCBI accession number NP_001180380.1)) and TMTC1.2 (TMTC1 isoform 2 (NCBI accession number NP_787057.2)). The open reading frame is indicated in *black*, and the different 5′-untranslocated regions are designated by *brown* (TMTC1.1) and *green* (TMTC1.2) *boxes*. Different 5′ primers (*P1–P4*) were designed to amplify specific isoforms using the same 3′ primer (*P5*). *C*, RNA was reverse-transcribed to cDNA followed by PCR with the TMTC1 isoform-specific primers. P1 and P2 are specific for TMTC1.1 (*lanes 1* and *2*), and P4 is specific for TMTC1.2 (*lane 4*). P3 is directed toward both isoforms (*lane 3*). PCR products were resolved by agarose gel electrophoresis with the nucleotide base pair markers (*kbp*) indicated to the *right*.

between 340 and 380 nm by a filter wheel. After stable baseline fluorescence had been established, carbachol and ATP (final concentration 100 μM for each) were added to the media to release intracellular calcium. Light emitted by Fura2 was collected by a cool SNAP ES digital camera, and all the obtained data were processed using SimplePCI software. Statistical analysis and areas under the curve calculations were completed using GraphPad Prism 4.0 software. The area under the curve was calculated by subtracting the baseline for each of the cells prior to the addition of carbachol. Once individual areas under the curve were obtained, the measurements were averaged for all cells in that treatment. The average calculated for the mock was set to 1.00, and the values of the treated cells were calculated relative to this number. Statistical significance was calculated using an unpaired *t* test. Cells analyzed in all Fura2 experiments were from at least five different plates collected on three separate days. Experiments with ionomycin were carried out in the same manner with the exception of calcium-free media being used during imaging.

RESULTS

TMTC1 and TMTC2 Are ER Resident Proteins—As adapter proteins commonly use clusters of TPR domains to modulate protein-protein interactions, we hypothesized that the ER might contain TPR domain-containing proteins, in addition to SEL1L and p58^{IPK} that contribute to the organization of the ER. Databases (SMART7 (25)) and a Regan lab TPR protein library (Yale University) (26) were queried with SignalP 3.0 to identify TPR proteins that were potentially targeted to the secretory pathway (27). TMTC1 (transmembrane and TPR repeat-containing protein 1 (NCBI accession number NP_787057.2)) and TMTC2 (NCBI accession number NP_689801.1) were identified as TPR-containing proteins with potential N-terminal signal sequences. These proteins were initially identified, but not characterized, in a large human sequencing study that identified opening reading frames from human cells (28, 29). *In silico* analysis of TMTC1 and TMTC2 indicated that each protein contained a potential N-terminal signal sequence and 10 C-terminal TPR domains (Fig. 1*A*).

Two TMTC1 isoforms are reported in the NCBI Protein Database with NCBI accession numbers NP_001180380.1 and NP_787057.2 for isoforms 1 and 2, respectively (30). TMTC1 splice variants present in HEK293T cells were determined by PCR using isoform-specific primers on a cDNA library generated from total mRNA. A PCR product was observed using the primers directed against regions of the TMTC1 isoform 2, whereas a product was not generated for isoform 1 (Fig. 1, *B* and *C*). qRT-PCR using a variety of primer sets failed to amplify a PCR product that would correlate with TMTC1 isoform 1. As

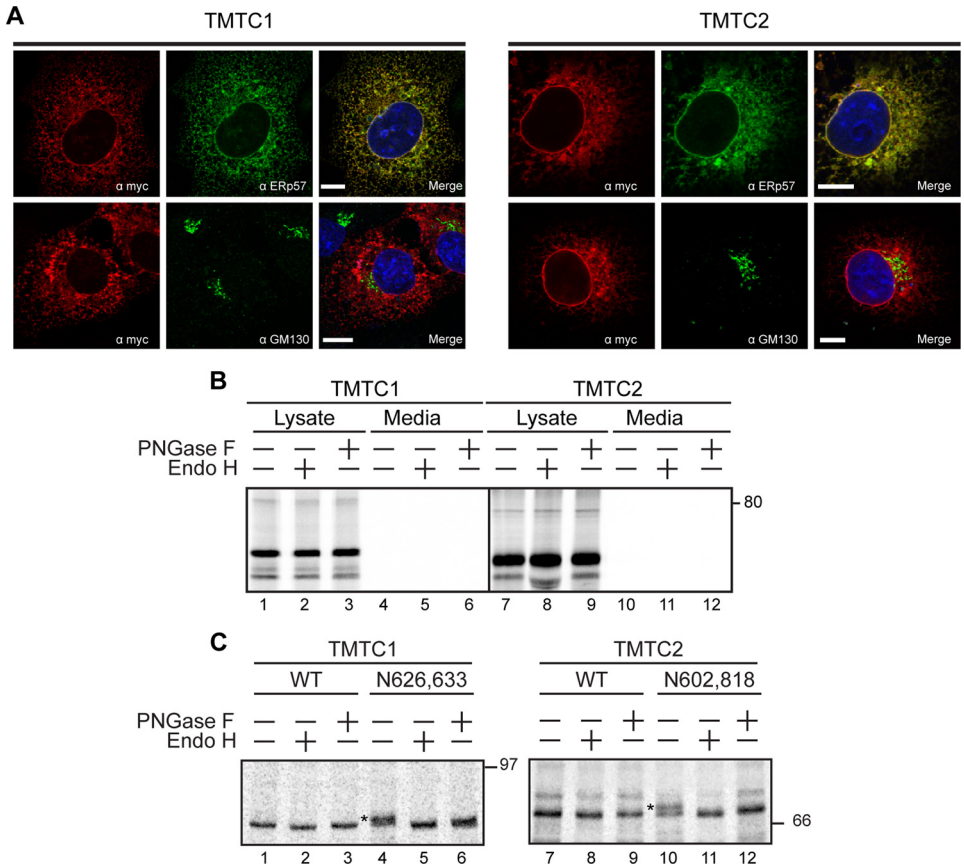

FIGURE 2. **TMTC1 and TMTC2 are ER-localized.** *A*, cellular localization of TMTC1 and TMTC2 was investigated by confocal microscopy. COS7 cells were transfected with TMTC1 or TMTC2 cDNA. Fixed cells were stained with Myc, ERp57 (*ER*), or GM130 (Golgi) antisera. Nuclei were visualized by DAPI staining (*blue*). *Scale bars* correspond to 10 μm. *B*, HEK293T cells were transfected with S-tagged TMTC1 or TMTC2 as indicated and radiolabeled for 1 h with [^{35}S]Cys/Met. Cells and media were collected. TMTC1 and TMTC2 from the media and lysed cells were affinity-purified using S-protein-agarose. Samples were then subjected to a glycosylation assay with either Endo H (*lanes 2, 5, 8,* and *11*) or PNGase F (*lanes 3, 6, 9,* and *12*) digestion as indicated. Reducing sample buffer was added, and the samples were analyzed by 7.5% SDS-PAGE. *C*, two *N*-linked glycosylation sites were introduced into TMTC1 (TMTC1$^{\text{Asn-626, Asn-633}}$) and TMTC2 (TMTC2$^{\text{Asn-602, Asn-818}}$). Added glycan positions are indicated by the *asterisks* in Fig. 1*A*. Samples were treated and digested as in *B*. Molecular mass markers are designated in kDa to the *right* for all SDS-PAGE panels.

only the TMTC1 isoform 2 was expressed in HEK293T cells, this isoform will be referred to as TMTC1.

TMTC1 and *TMTC2* cDNAs were subcloned into mammalian expression vectors encoding a C-terminal Myc tag, and their cellular localization was determined by confocal immunofluorescence microscopy. COS7 cells were transfected with either TMTC1-Myc or TMTC2-Myc, and staining was compared against an ER (ERp57) or Golgi (GM130) marker (Fig. 2*A*). Both TMTC1 and TMTC2 co-localized with ERp57, although co-localization was not observed with GM130, suggesting that TMTC1 and TMTC2 are both ER resident proteins.

Secretory proteins are commonly modified in the ER with *N*-linked glycans at the consensus site Asn-Xaa-(Ser/Thr). TMTC1 and TMTC2 both possess a single *N*-linked glycosylation consensus site (Fig. 1*A*); therefore, a glycosylation assay was used to further analyze ER targeting and localization. As the molecular mass of an *N*-linked glycan is ~2.5 kDa, the removal of *N*-linked glycans by glycosidase treatment results in a corresponding increase in mobility for the deglycosylated protein. Endo H trims the high mannose glycans encountered in the ER, and PNGase F removes complex glycans acquired in the Golgi in addition to high mannose glycans.

HEK293T cells transfected with TMTC1 or TMTC2 containing a C-terminal S tag were pulsed with [^{35}S]Met/Cys for 60 min. Cell lysate and media fractions were affinity-precipitated with S-protein-agarose beads followed by glycosidase treatment. Shifts upon glycosidase treatment were not observed for either TMTC1 or TMTC2 indicating that neither protein appeared to be glycosylated (Fig. 2*B*). As not all glycosylation sites are efficiently recognized and modified, two *N*-linked glycosylation sites were introduced to the C-terminal portion of TMTC1 (TMTC1$^{\text{Asn-626, Asn-633}}$) and TMTC2 (TMTC2$^{\text{Asn-602, Asn-818}}$) (Fig. 1*A*, see *asterisks*). These constructs migrated slower than the wild type constructs, and their treatment with PNGase F produced faster migrating proteins indicating that TMTC1$^{\text{Asn-626, Asn-633}}$ and TMTC2$^{\text{Asn-602, Asn-818}}$ were both modified with *N*-linked glycans (Fig. 2*C*). A similar increase in mobility was observed upon Endo H treatment indicating that the carbohydrates were high mannose glycoforms. Therefore, the cellular distribution for TMTC1 and TMTC2 and the glycosylation profiles for the glycan addition mutants are consistent with TMTC1 and TMTC2 residing in the ER.

TMTC1 and TMTC2 Are Up-regulated by Redox Stress—Proteins that reside in the secretory pathway are frequently

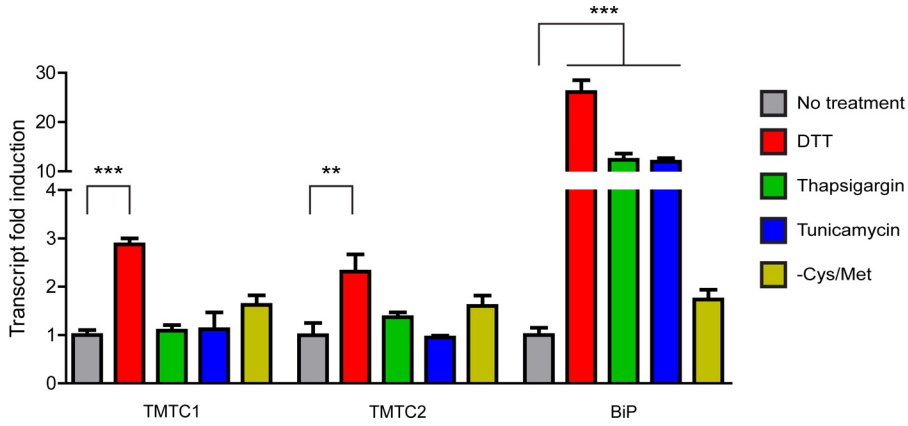

FIGURE 3. **TMTC1 and TMTC2 are up-regulated by redox stress.** HEK293T cells were treated with regular growth media or media containing 5 mM DTT, 1 μM thapsigargin, 5 μg/ml tunicamycin, or media lacking Cys and Met (−Cys/Met) for 8 h prior to RNA purification. RNA was reverse-transcribed to cDNA followed by qRT-PCR with appropriate primers, and changes in gene expression were calculated using β-actin as a reference. Statistical significance between treatment groups was determined using one-way analysis of variance followed by Tukey's multiple comparison tests; ** and *** indicate p values of less than 0.01 and 0.001, respectively. *Error bars* represent standard deviation from at least three independent experiments.

transcriptionally up-regulated by stress as their functions can help to alleviate stress (31). To determine whether the *TMTC1* and *TMTC2* genes are transcriptionally regulated by ER stress, HEK293T cells were exposed to different ER stress conditions. Cells were subjected to redox stress (dithiothreitol, DTT), calcium depletion (thapsigargin), *N*-glycan synthesis inhibition (tunicamycin), or amino acid starvation (−Cys/Met). RNA was harvested from cells followed by reverse transcription to generate cDNA, and changes in gene expression were measured by qRT-PCR. *TMTC1* and *TMTC2* gene expression was increased with DTT treatment by 3.9- and 2.3-fold, respectively (Fig. 3). However, thapsigargin, tunicamycin, or amino acid starvation did not produce a significant increase in gene expression of *TMTC1* or *TMTC2*, although the transcription of *BiP* was significantly stimulated by DTT, thapsigargin, and tunicamycin. Thus, only redox stress increased the transcription of *TMTC1* and *TMTC2*.

TMTC1 and TMTC2 Are ER Membrane Proteins with Luminal Oriented TPR Domains—Analysis of the TMTC1 and TMTC2 protein sequences with ΔG prediction demonstrated that TMTC1 and TMTC2 contained 9 and 10 hydrophobic segments, respectively, that could potentially serve as transmembrane domains to create polytopic membrane proteins (Fig. 1*A*) (19). Alkaline extraction of membrane fractions was performed to separate membrane and soluble forms of proteins following centrifugation to determine whether TMTC1 and TMTC2 are integral membrane proteins (32, 33).

HEK293T cells were transfected with either TMTC1 or TMTC2, and proteins were radiolabeled with [^{35}S]Met/Cys for 60 min. Cells were homogenized in isotonic buffer, and fractions were separated by centrifugations. TMTC1 and TMTC2 were found in the total membrane and nuclear fractions (Fig. 4*A*). The nuclear localization of TMTC1 and TMTC2 is likely explained by the contiguous nature of the ER and nuclear membrane prohibiting their separation as the ER proteins calnexin and calreticulin were also in the nuclear fractions. Alkaline extraction of the total membrane fractions followed by centrifugation found TMTC1 and TMTC2 exclusively in the membrane pellet. This profile was observed for the ER membrane protein calnexin and not its soluble paralogue calreticulin, which largely accumulated in the supernatant. Therefore, both TMTC1 and TMTC2 are integral membrane proteins.

Because TMTC1 and TMTC2 are membrane proteins, a trypsin protection assay was employed to determine whether their C-terminal TPR domains are positioned in the ER lumen or the cytoplasm. HEK293T cells were transfected with either TMTC1 or TMTC2 constructs containing C-terminal S tags and pulsed with [^{35}S]Met/Cys for 60 min followed by homogenization and isolation of ER-enriched microsomes. Isolated microsomes were resuspended in an isotonic buffer, and aliquots were treated with Triton X-100 and trypsin as indicated. Affinity purification using S-agarose beads allowed the isolation of proteins containing a protected C terminus. Trypsin treatment produced discrete TMTC1 and TMTC2 fragments of 62.5 and 51.6 kDa, respectively (Fig. 4*B*, compare *lanes 5* and *6* and *9* and *10*). As the TPR domains and S tags are both at the C termini, this demonstrated that the TPR domains of TMTC1 and TMTC2 were positioned in the ER lumen. Combined with the modification of the glycosylation sites added to the TPR-rich regions (Fig. 2*C*), these results demonstrated that the TPR domains for both of the membrane proteins TMTC1 and TMTC2 were facing the ER lumen.

TMTC1 and TMTC2 Associate with SERCA2B—To identify binding partners of TMTC1 and TMTC2, a shotgun liquid chromatography-mass spectrometry/mass spectrometry (LC-MS/MS) approach was used. Cells expressing either TMTC1 or TMTC2 with a C-terminal S tag were homogenized, and ER-derived microsome fractions were isolated. Proteins associated with TMTC1 and TMTC2 were isolated using the S-protein-agarose beads and resolved by SDS-PAGE. The gels were subjected to either silver staining or in-gel trypsin digestion followed by LC-MS/MS analysis (Fig. 5*A*). The proteins associated with the S-tagged proteins obtained from the LC-MS/MS analysis are listed in supplemental Table S1. The LC-MS/MS results indicated possible interactions for TMTC1 and TMTC2 with SERCA2B, calnexin, BiP, and the glucosidase II α subunit.

To verify the interactions identified using the mass spectrometry approach, HEK293T cells were transfected with the C-terminal S-tagged TMTC1 or TMTC2, followed by affinity purification and immunoblotting against endogenous associ-

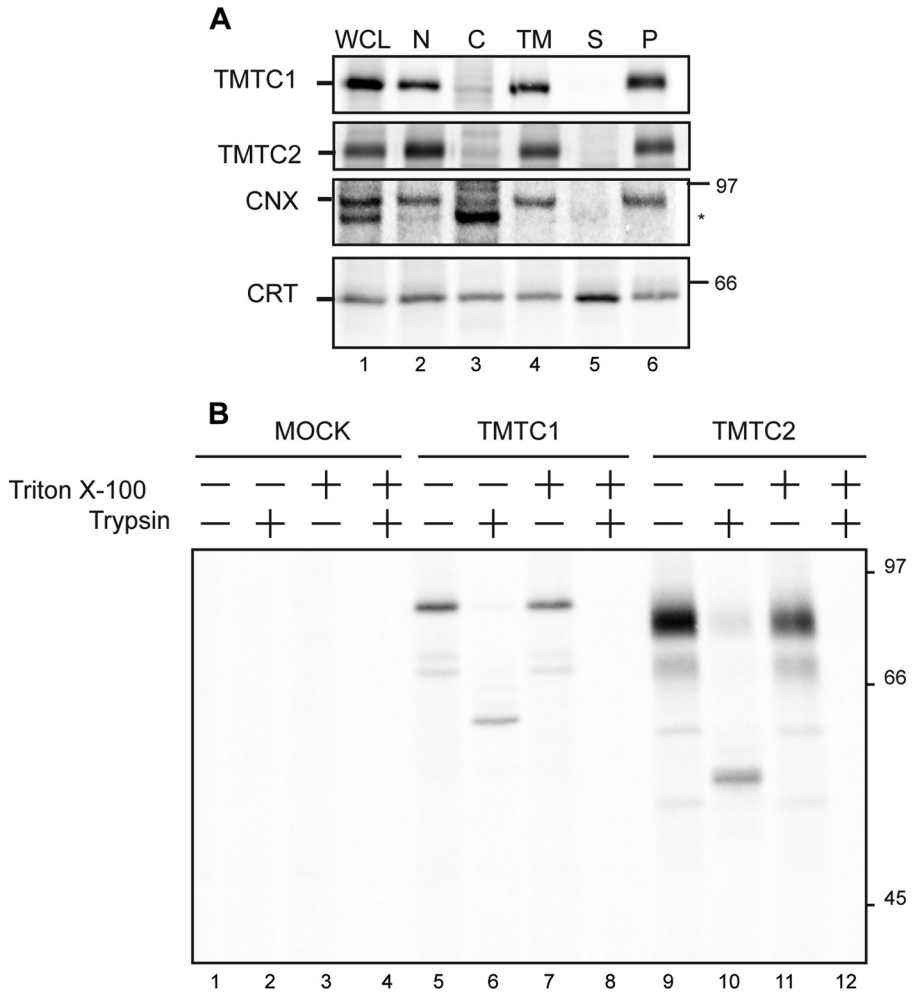

FIGURE 4. **TMTC1 and TMTC2 are ER membrane proteins with their TPR domains facing the ER lumen.** *A*, HEK293T cells expressing S-tagged TMTC1 or TMTC2 were radiolabeled for 1 h followed by homogenization, fractionation, and alkaline extraction. The fractions collected were whole cell lysate (*WCL*), nucleus (*N*), cytosol (*C*), total membrane (*TM*), supernatant (*S*) ,and pellet (*P*) fractions upon alkaline extraction of the total membrane. Samples were resolved by reducing 7.5% SDS-PAGE. *B*, TMTC1-S tag or TMTC2-S tag was expressed in HEK293T cells. After radiolabeling for 1 h, cells were homogenized, and microsomes were purified by ultracentrifugation and then resuspended in homogenization buffer. Aliquots of the ER microsomes were incubated for 10 min at 27 °C without (*lanes 1*, *5*, and *9*) or with 0.1% Triton X-100 and 10 μg of trypsin (*lanes 4, 8,* and *12*) as indicated. TMTC1 or TMTC2 was affinity-purified with S-protein-agarose beads. Samples were resolved on a reducing 9% SDS-PAGE. *CNX*, calnexin; *CRT*, calreticulin.

ated proteins. Both TMTC1 and TMTC2 readily interacted with SERCA2B, a polytopic ER calcium pump responsible for calcium uptake from the cytoplasm into the ER (Fig. 5*B*). TMTC2, but not TMTC1, interacted with calnexin. Calnexin is a carbohydrate-binding chaperone of the ER membrane that associates with maturing glycoproteins that possess monoglucosylated glycans (34). The TMTC2-calnexin interaction appeared to be specific because TMTC2 did not interact with calreticulin, the soluble paralog of calnexin, or the calnexin-associated oxidoreductase ERp57 (Fig. 5*B*). The interaction between calnexin and TMTC2 was reduced but not abolished by glucosidase inhibition with *N*-butyl-deoxynojirimycin even though TMTC2 was not glycosylated (Fig. 5*C*). These results suggested that an additional glycosylated component might be involved in TMTC2 binding to calnexin. Despite being identified by the mass spectrometry results (supplemental Table S1), no interaction between TMTC1 and TMTC2 with either BiP or the glucosidase II α subunit was observed (Fig. 5*B*).

To determine the approximate size of the TMTC1 and TMTC2 complexes, velocity centrifugation was performed. HEK293T cells were transfected with either S-tagged TMTC1 or TMTC2. Cells were lysed in Triton X-100, and cell lysates were layered on a 10–40% linear sucrose gradient followed by centrifugation. TMTC1 and TMTC2 were exclusively found in the larger fractions indicating that both proteins resided in large protein complexes (Fig. 5*D*, *fractions 7–10*). The SERCA2B sedimentation profile overlapped with the TMTC1 and TMTC2 profiles, although SERCA2B was also found in lighter fractions absent of TMTC1 and TMTC2 (Fig. 5*D*, *fractions 5* and *6*). Although calnexin was predominantly localized to smaller sized fractions (Fig. 5*D*, *fractions 1–4*), a portion was also observed in the TMTC1 and TMTC2 fractions. Collectively, these results indicate that TMTC1 and TMTC2 are found in large protein complexes that include SERCA2B, as well as calnexin for TMTC2.

To determine whether the interactions with TMTC1 and TMTC2 involved their TPR domains, the C-terminal TPR-rich portions of TMTC1 ($TMC1^{TPR}$) and TMTC2 ($TMC2^{TPR}$) were targeted to the ER in HEK293T cells using the signal sequence of BiP and a C-terminal S tag followed by an ER KDEL retention

sequence to support ER residency. TMTC1^{TPR} and TMTC2^{TPR} were both efficiently targeted to and retained in the ER as observed by confocal immunofluorescence microscopy (Fig. 6*A*) and the absence of the appearance of the constructs in the cell media (data not shown). TMTC1^{TPR} and TMTC2^{TPR} maintained their interaction with SERC2B, suggesting that these

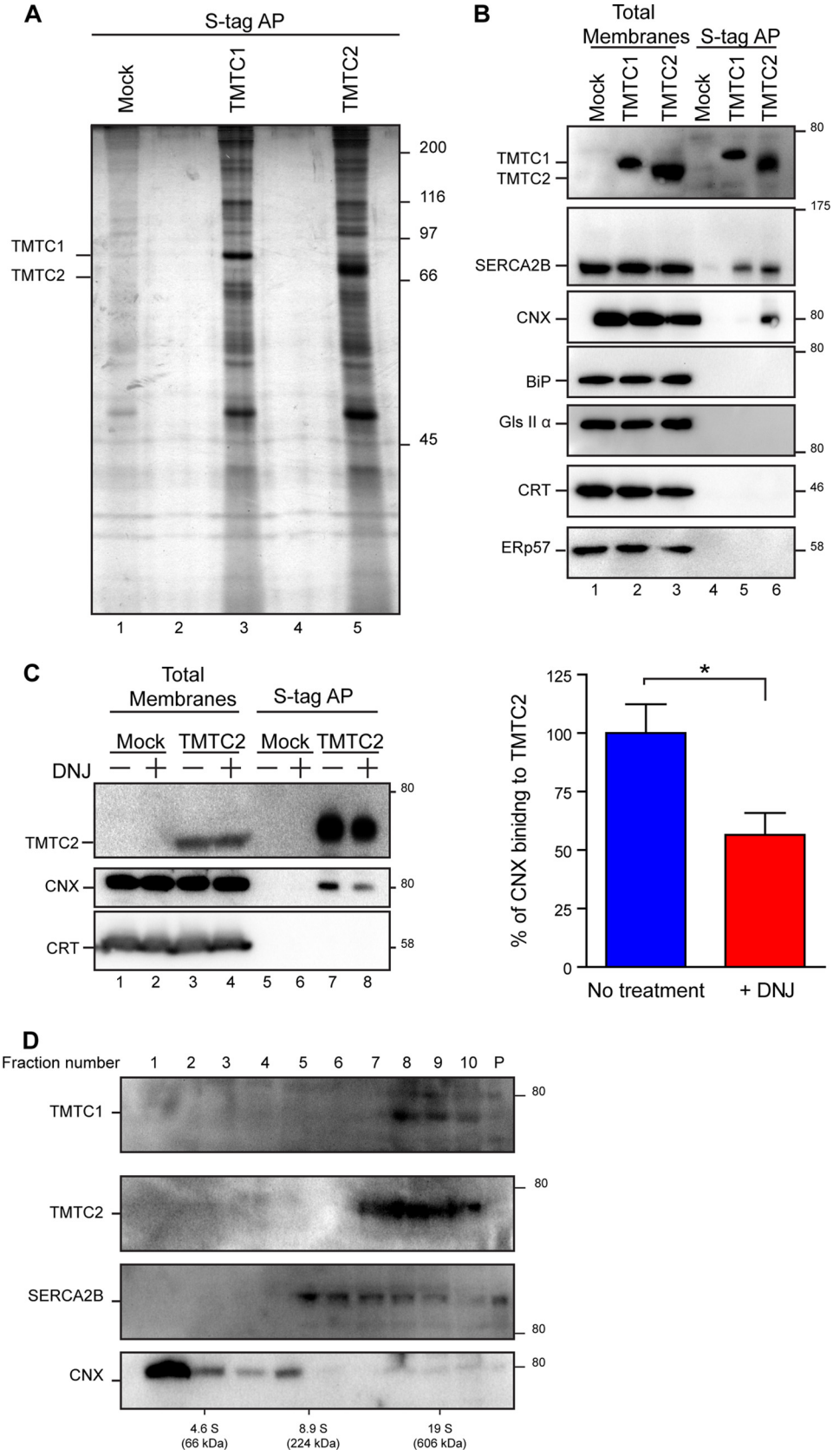

interactions were mediated through the TPR domains of TMTC1 or TMTC2. In contrast, $TMTC2^{TPR}$ did not associate with calnexin, implying that this interaction required the transmembrane domain of TMTC2 (Fig. 6*B*). Thus, the TPR domains of TMTC1 and TMTC2 were utilized to mediate the interactions with SERCA2B.

TMTC1 and TMTC2 Alter Cytoplasmic Calcium Levels—As TMTC1 and TMTC2 both interact with SERCA2B, live cell calcium measurements were used to elucidate the impact of TMTC1 and TMTC2 on calcium regulation. Initially, cytoplasmic calcium levels were monitored after the overexpression of TMTC1 or TMTC2. Green fluorescent protein (GFP) was fused to the C termini of TMTC1 ($TMTC1^{GFP}$) and TMTC2 ($TMTC2^{GFP}$) to mark efficiently transfected cells for analysis (Fig. 7*A*). Cells were incubated with Fura2 acetoxymethyl ester, a membrane-permeable fluorophore that is rendered membrane-impermeable by cytoplasmic esterases. The treatment of cells with ATP and carbachol releases intracellular calcium stores, as carbachol is a noncleavable acetylcholine analogue that stimulates muscarinic receptors at the plasma membrane resulting in the downstream release of calcium from the ER via the inositol trisphosphate receptor (35, 36).

Cell expressing $TMTC1^{GFP}$ or $TMTC2^{GFP}$ and treated with ATP and carbachol showed calcium responses that reached peak levels earlier than nontransfected cells (Fig. 7*B*). Nevertheless, a 33.8, 45.2, and 30.4% decrease in calcium release was observed in cells expressing either $TMTC1^{GFP}$,$TMTC2^{GFP}$, or both compared with nontransfected cells, respectively. These results suggest that TMTC1 and TMTC2 affect calcium homeostasis, possibly by modifying the calcium sequestering capacity of SERCA2B to decrease the duration of the calcium signal. No synergy between TMTC1 and TMTC2 was observed when both proteins were expressed together.

Intracellular calcium release can also be stimulated by addition of calcium ionophores such as ionomycin, which promote release mostly from intracellular stores when the exposure is performed in the absence of extracellular calcium. Therefore, cells expressing $TMTC1^{GFP}$ or $TMTC2^{GFP}$, bathed in calcium-free media and exposed to ionomycin, had a 20.2 and a 27.4% reduction in calcium release, respectively (Fig. 7, *C* and *D*). This implies that intracellular calcium stores were reduced by overexpression of $TMTC1^{GFP}$ or $TMTC2^{GFP}$.

Next, the effect of TMTC1 or TMTC2 knockdown on cytoplasmic calcium levels was investigated. TMTC1 or TMTC2 was knocked down by transfecting HEK293T cells with a polycistronic plasmid that expressed an shRNA directed toward transcripts for either TMTC1 or TMTC2, as well as a cytoplasmic localized GFP to mark transfected cells. To verify knockdown efficiencies, RNA was harvested from HEK293T cells 24 h post-transfection, and changes in gene expression were measured by qRT-PCR (Fig. 8*A*). Fluorescence-activated cell sorting of GFP-expressing cells was used to measure transfection efficiency of the different shRNA constructs. TMTC1 shRNA1 and TMTC2 shRNA3 achieved the maximum knockdown of 55 and 48%, respectively, in a cell mixture of transfected and nontransfected cells. These shRNA constructs were used for further analysis of the effects on calcium measurements. Because cytoplasmic GFP was also expressed from the shRNA-encoding plasmid, transfected and nontransfected cells were readily distinguishable by microscopy. Knockdown of either TMTC1, TMTC2, or both resulted in a 33.1, 64.1, or 71.0% increase in carbachol-stimulated ER calcium release, respectively (Fig. 8*B*). Although peak calcium levels were not greatly affected by knockdown of either molecule, calcium release was enhanced, especially after TMTC2 knockdown, which prolonged the response, suggesting that it promoted greater calcium influx. Collectively, these results indicate that overexpression of TMTC1 or TMTC2 decreases stimulated calcium release, whereas their knockdown, especially for TMTC2 or both TMTC1 and TMTC2 combined, enhanced calcium increases into the cytoplasm supportive of a role for TMTC1 and TMTC2 in calcium regulation.

DISCUSSION

We identified and characterized two novel TPR-rich ER proteins, TMTC1 and TMTC2. They share a 54% similarity and 27% identity in the amino acid sequence, suggestive of a common evolutionary origin (21). Basic Local Alignment Search Tool analysis indicated that TMTC1 and TMTC2 homologues are conserved in the chordata phylum and are absent in lower eukaryotes such as yeast as is their most prominent associated protein SERCA2B (37). Published microarray data shows that TMTC1 and TMTC2 are transcribed in a wide range of human tissues (38). TMTC1 and TMTC2 are divided into two regions that appear to create two functionally distinct domains, an N-terminal hydrophobic region and a C-terminal domain that contains multiple TPR clusters (Fig. 1*A*).

Alkaline extraction of total membrane preparations demonstrated that TMTC1 and TMTC2 are integral membrane pro-

FIGURE 5. **TMTC1 and TMTC2 interact with SERCA2B.** *A*, HEK293T cells were transfected as indicated and homogenized prior to purification of microsomes by ultracentrifugation. TMTC1 or TMTC2 was isolated with its associated factors from microsomes in MS buffer using S-protein-agarose affinity precipitation. A portion of the samples was loaded onto SDS-PAGE and silver-stained to verify enrichment of putative binding partners. A separate portion of the affinity-purified sample was run on a short SDS-PAGE before excision of the sample and in-gel trypsin digestion. Tryptic peptides were injected into an LC-MS/MS instrument followed by peptide identification. *B*, HEK293T cells expressing TMTC1 or TMTC2 were harvested in homogenization buffer. A portion of the cell homogenate was subjected to ultracentrifugation and resuspended in reducing sample buffer. This was considered the total membrane fraction. An excess of MNT was added to an equal amount of cell homogenate and subjected to S-protein-agarose affinity precipitation. Proteins were detected by immunoblotting with appropriate antisera directed against the S tag epitope, SERCA2B, calnexin (*CNX*), BiP, glucosidase II subunit α (*Gls II* α), calreticulin (*CRT*), and ERp57. *C*, HEK293T cells were treated with DNJ for 4 h prior to homogenization where indicated, and samples were processed as in *B*. Quantification of the TMTC2 and calnexin interaction was calculated as described above, and *error bars* represent standard deviation of three independent experiments. Statistical significance between treatment groups was determined by an unpaired *t* test, and the measurements designated (*) have a *p* value of 0.0233. *D*, HEK293T cells were transfected as indicated above. Cells were lysed in MNT, and samples were layered on top of a continuous 10–40% sucrose gradient in MNT buffer prior to ultracentrifugation. Fractions were collected from the top of the gradient, and proteins were precipitated with trichloroacetic acid. Immunoblotting was then performed with appropriate antisera as described above. Sizing of detected complexes was estimated by comparison with the following standards designated at the *bottom* of the immunoblots: bovine serum albumin (4.6 S, 66 kDa); β-amylase (8.9 S, 200 kDa); and bovine thyroglobulin (19 S, 669 kDa).

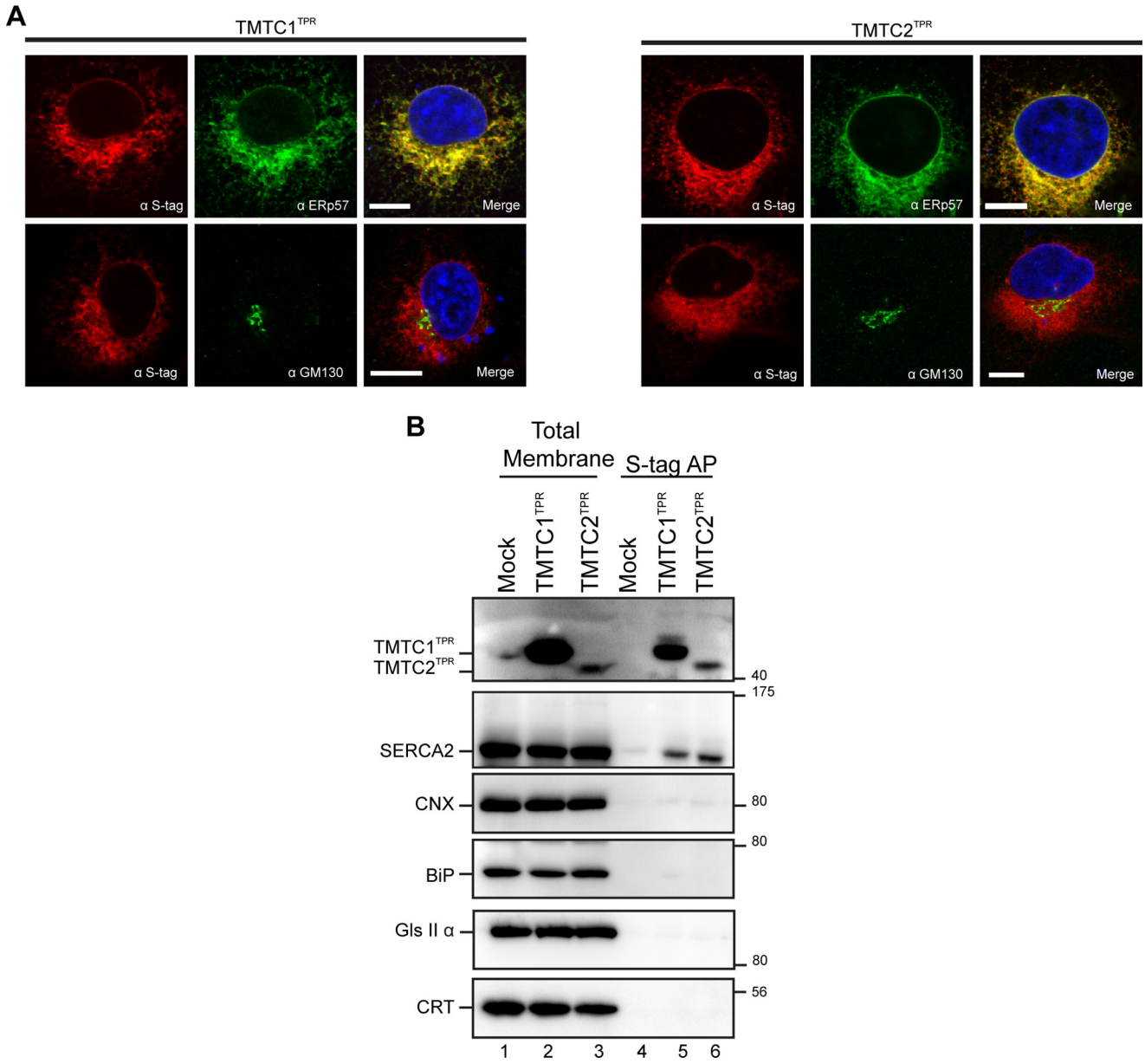

FIGURE 6. **TPR domains of TMTC1 and TMTC2 are sufficient to interact with SERCA2B.** *A*, COS7 cells were transfected with TMTC1^{TPR} and TMTC2^{TPR}, and cells were treated and stained as described in Fig. 2*A*. *B*, HEK293T cells were transfected with either TMTC1^{TPR} or TMTC2^{TPR}, harvested, and homogenized. Total membrane fractionation and affinity precipitation were performed as described in Fig. 5*B*. Proteins were detected with appropriate antisera against the S tag, SERCA2B, calnexin (*CNX*), BiP, glucosidase II subunit α (*Gls II α*), and calreticulin (*CRT*).

teins. ΔG analysis predicts that the N termini of TMTC1 and TMTC2 have 10 and 11 potential transmembrane domains, respectively. A negative ΔG associated with a high probability of membrane integration was calculated for five (TMTC1) and three (TMTC2) of these hydrophobic segments. Hydrophobic domains with a positive ΔG frequently insert into membranes upon stabilization by efficiently inserted transmembrane domains (19). Therefore, TMTC1 and TMTC2 appear to be polytopic membrane proteins with their hydrophobic N termini providing a long stretch of multiple transmembrane segments. The presence of a number of hydrophilic and charged residues within some of the hydrophobic domains of TMTC1 and TMTC2 imply that these residues could be used for intramembrane interactions, such as the TMTC2-calnexin interaction.

The single natural *N*-glycosylation site present in the N-terminal hydrophobic portion of either TMTC1 or TMTC2 was not modified as probed by a glycosidase mobility shift assay. Lack of apparent glycosylation could be due to positioning of the consensus sites in the cytoplasm or being too close to the membrane for recognition by the oligosaccharyltransferase (39). Alternatively, the shift caused by glycosidase treatment and the removal of a single glycan might be too slight to be visualized for these large hydrophobic proteins. However, ER targeting was verified by placing efficiently modified glycosylation sites in the C-terminal TPR-rich regions of both TMTC1 and TMTC2 and by confocal immunofluorescence microscopy.

The glycosylation of sites added to the TPR regions of TMTC1 and TMTC2, combined with the trypsin protection of

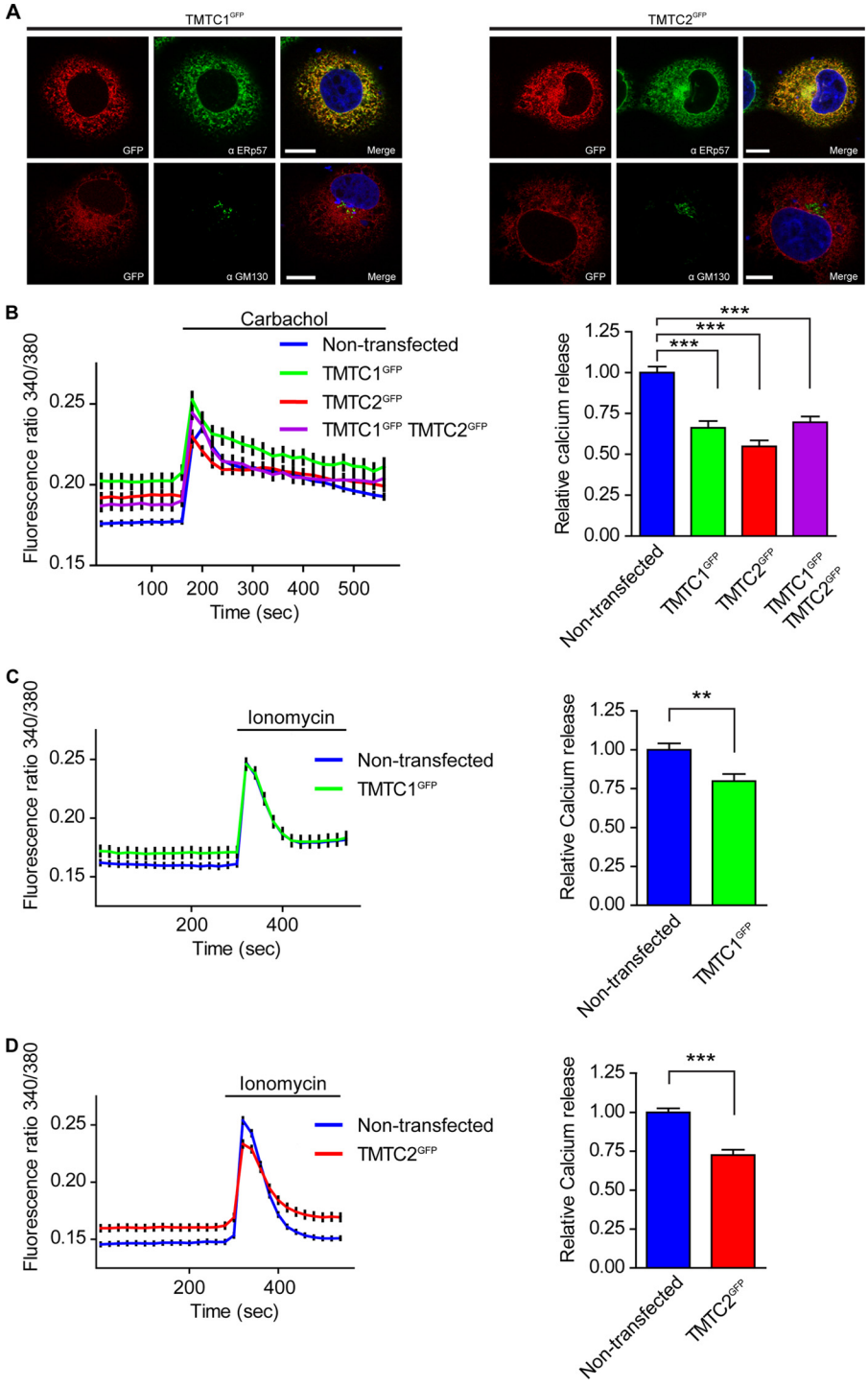

FIGURE 7. **Overexpression of TMTC1 and TMTC2 decreased stimulated calcium release.** *A*, COS7 cells were transfected with TMTC1^{GFP} or TMTC2^{GFP}, treated, stained, and analyzed as in Fig. 2*A*. *B*, HEK293T cells transfected with TMTC1^{GFP}, TMTC2^{GFP}, or co-transfected with both were incubated with Fura2 acetoxymethyl ester followed by incubations in fresh media. Changes in cytoplasmic calcium were determined by measuring the ratio of fluorescence emission after excitation at 340 and 380 nm. Basal calcium levels were recorded to create a stable baseline before calcium release was stimulated with the addition of 100 μM ATP and 100 μM carbachol to the media (see *bar*). A total of 386, 91, 103, and 106 cells was measured for nontransfected control, TMTC1^{GFP}, TMTC2^{GFP}, and co-transfection of TMTC1^{GFP} with TMTC2^{GFP}, respectively. *Error bars* represent mean ± S.E. The area under the curve is relative to the total amount of calcium released from the ER upon stimulation (*bar graph*). Statistical significance between nontransfected cells and either TMTC1^{GFP}, TMTC2^{GFP}, or the TMTC1^{GFP} TMTC2^{GFP} co-transfection was calculated by using an unpaired *t* test. Measurements designated *** had a *p* value of <0.0001. *Error bars* represent mean ± S.E. *C*, HEK293 cells were transfected with TMTC1^{GFP}, and live cell calcium measurements were performed as in *B*. Basal calcium levels were recorded before 2 μM ionomycin (see *bar*) was added to media to release intracellular calcium. All recordings were performed in calcium-free media to prevent interference from extracellular calcium. A total of 130 and 78 cells were analyzed for nontransfected control and TMTC1^{GFP}, respectively. The area under the curve is relative to the total amount of calcium released from the ER upon stimulation (*bar graph*). Statistical significance between nontransfected cells and TMTC1^{GFP} was calculated using an unpaired *t* test; measurements designated ** have a *p* value of 0.0022. *Error bars* represent mean ± S.E. *D*, HEK293 cells were transfected with TMTC2^{GFP}, and live cell calcium measurements were performed as in *C*. A total of 140 and 100 cells were analyzed for nontransfected control and TMTC2^{GFP}, respectively. Statistical significance between nontransfected cells and TMTC2^{GFP} was calculated by using an unpaired *t* test. Measurements designated ** have a *p* value of >0.0001. *Error bars* represent mean ± S.E.

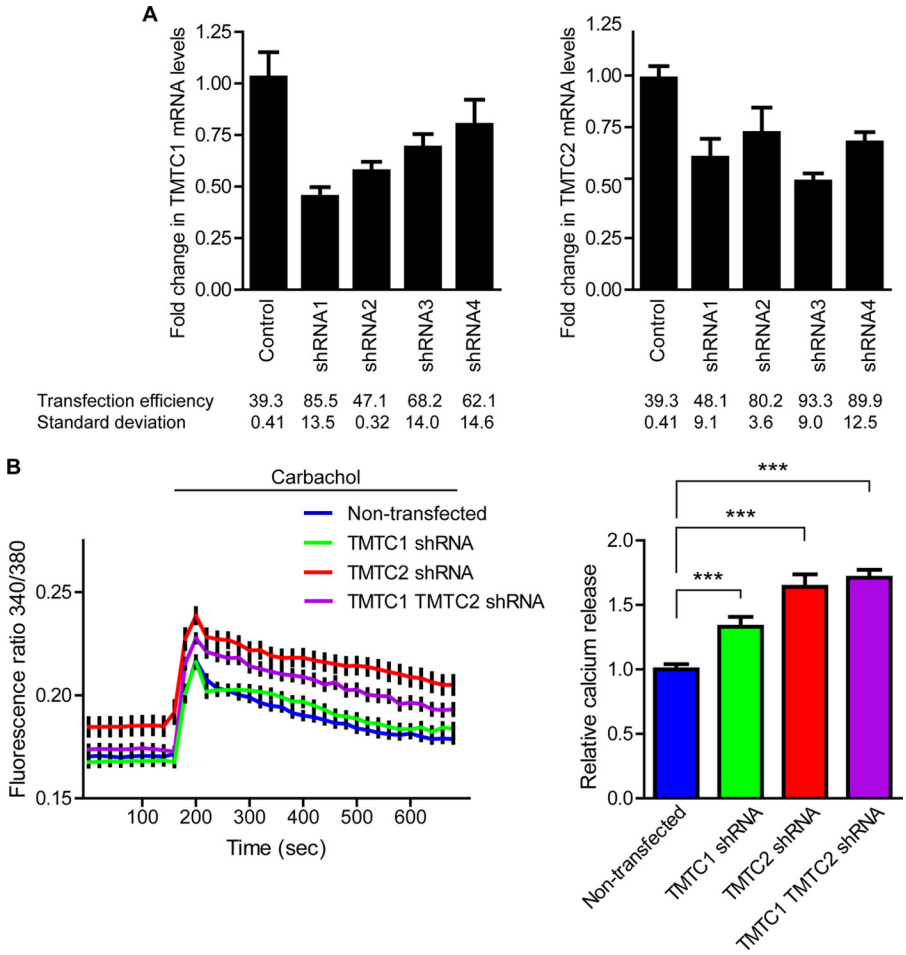

FIGURE 8. **Knockdown of TMTC1 and TMTC2 increased stimulated calcium release.** *A*, HEK293T cells were transfected with polycistronic plasmids that expressed shRNA (directed toward TMTC1 or TMTC2 transcripts) and cytoplasmic GFP. RNA was purified from HEK293T cells, and the RNA was reverse-transcribed to cDNA followed by qRT-PCR. Changes in gene expression were measured using *β-actin* as a reference gene. Fold reduction in TMTC1 or TMTC2 mRNA abundance was compared with mock-transfected cells. Four different shRNAs and a scrambled negative control were tested for knockdown of TMCT1 and TMTC2. *Error bars* indicate standard deviation from three independent experiments. HEK293T cells transfected with the different shRNA constructs and GFPs were also analyzed and scored as nontransfected or transfected based on GFP fluorescence using flow cytometry. A total of 5,000 cells were counted per experiment, and standard deviations were calculated from at least two separate experiments. *B*, HEK293T cells were transfected with either TMTC1 shRNA1, TMTC2 shRNA3, or co-transfection with TMTC1 shRNA1 and TMTC2 shRNA3. Live cell calcium measurements were performed as in Fig. 7*B*. Once a stable baseline was obtained, 100 μM ATP and 100 μM carbachol was added to the media (see *bar*). A total of 297, 137, 115, and 208 cells were measured for nontransfected control, TMTC1 shRNA1, TMTC2 shRNA3, and the co-transfection of TMTC1 and TMTC2 shRNAs, respectively. *Error bars* represent mean ± S.E. The area under the curve is relative to the total amount of calcium released from the ER upon stimulation. Statistical significance between nontransfected cells and either TMTC1 shRNA1 or TMTC2 shRNA3 was calculated by using an unpaired *t* test. Measurements designated *** have a *p* value of <0.0001. *Error bars* represent mean ± S.E.

the C-terminal domains from isolated membranes, placed the TPR domains within the ER lumen for both TMTC1 and TMTC2. The trypsin-protected fragments of 63 kDa (TMTC1) and 52 kDa (TMTC2) corresponded to the complete C-terminal TPR domains (Fig. 1*A*). UniProt predicted that TMTC1 has a total of 10 TPR domains organized into clusters of seven and three, while TMTC2 has 10 total TPR domains found in clusters of four and six. In contrast, analysis of TMTC1 by TPR domain prediction software TPRpred did not recognize the second and sixth TPR domains of TMTC1 as *bona fide* TPR domains. The space between the seventh and eighth TPR domains in TMTC1, which was not identified by UniProt, was predicted to be an additional TPR domain by TPRpred; UniProt and TPRpred predictions are in strong agreement for TMTC2. The only discrepancy between the analyses was that TPRpred did not recognize the first TPR motif of TMTC2. The differences in organization of the TPR domains of TMTC1 and TMTC2 could have implications for their functions.

TPR domains are found in proteins across species and organelles and participate in a plethora of activities, including protein folding, post-translational modification, translocation, and signal transduction. Clusters of TPR domains form discrete domains that nucleate protein-protein interactions (9, 11, 40). Sucrose sedimentation analysis suggested that both TMTC1 and TMTC2 resided in large molecular weight complexes. SERCA2B was the most prominent associated proteins for both TMTC1 and TMTC2, and this interaction was mediated through the TPR domains as the association persisted with a soluble construct composed solely of the TPR-rich C-terminal region. The dependence of the TPR domains of TMTC1/TMTC2 for the interactions with SERCA2B was unexpected given the hydrophobic nature of

TMTC1/TMTC2 and SERCA2B, and the small portion of SERCA2B that is exposed to the ER lumen. It cannot be ruled out at this time that the TMTC1 or TMTC2 interaction with SERCA2B is mediated through an additional protein in the large complex.

The carbohydrate-binding ER chaperone, calnexin, was also found to interact with the nonglycosylated TMTC2 but not TMTC1. Binding was reduced by 50% in the presence of glucosidase inhibition. Calnexin did not interact with the soluble TPR domain construct of TMTC2. The interaction could be mediated through the transmembrane segments of SERCA2B and calnexin (a type I membrane protein) as calnexin has been proposed to monitor proteins within the ER bilayer (41). Alternatively, an additional glycosylated substrate such as SERCA2B may be involved in the interaction between TMTC2 and calnexin, as calnexin is known to associate with SERCA2B (42).

TMTC1 and TMTC2 overexpression reduced the amount of calcium released from the ER after stimulation with carbachol and ATP. This reduction might be caused by a decrease in the total amount of calcium stored in the ER, implying a defect in calcium uptake and/or storage. This is consistent with the observed higher baseline calcium values, especially in cells overexpressing TMTC2. Elevated baselines and reduced calcium release was also seen in studies using ionomycin implying that overexpression of TMTC1 or TMTC2 disrupts calcium homeostasis in these cells. It is unclear how these proteins might interfere with calcium ER levels, although SERCA2B is likely a target, given the evidence of direct interaction between these two molecules.

In contrast, knockdown of TMTC1 and TMTC2 caused an increase in the calcium response to the same agonists. Although the amplitude of the peak response was not higher, it was longer, especially after TMTC2 knockdown. An interpretation of these results is that the knockdown of TMTC2 promotes greater calcium influx, possibly caused by an initial larger calcium release and robust activation of the stored calcium entry mechanism. The other interpretation of the results, that knockdown of TMTC1 or TMTC2 reduces the capacity for SERCA2B to sequester cytoplasmic calcium, is not supported by the comparable amplitude of the calcium rise induced by the agonists. The observation that no additive effect was observed with either co-expression or co-knockdown of both TMTC1 and TMTC2 implies that TMTC1 and TMTC2 do not act synergistically. It is worth noting that in both overexpression and knockdown studies, TMTC2 gave a stronger response than TMTC1, which may be attributed to the interaction between TMTC2 and calnexin. Future studies should address the role of calnexin on the function of TMTC2.

The interaction between calnexin and SERCA2B can be modified by reversible post-translational phosphorylation or palmitoylation of calnexin (8, 42). Phosphorylation of the C-terminal cytoplasmic tail of calnexin is believed to reduce sequestering by SERCA2B, whereas palmitoylation of calnexin is proposed to increase SERCA2B activity. Because knockdown of TMTC2 increased calcium release, it is possible that this is accompanied by changes in post-translational modifications of calnexin. Furthermore, the decreased interaction between TMTC2 and calnexin caused by inhibition of glucosidase could be due to changes in post-translational modifications on either SERCA2B or calnexin (Fig. 5*C*). Collectively, these modifications allow for a dynamic control of calcium sequestering adjustable to the current needs of the cell.

An RNAi-based screen for proteins that effect protein trafficking found that knockdown of TMTC1 caused a reduction in the level of a viral glycoprotein localized to the cell surface and that the Golgi appeared dispersed (43). In our study, knockdown of TMTC1 or TMTC2 in HeLa cells did not cause a significant defect in either ER or Golgi morphology. This discrepancy could be caused by differences in the cell lines employed (44).

The identification of TMTC1 and TMTC2 as ER membrane adapters and their interactions with SERCA2B highlights the exquisite organization and functional regulation of the ER and its components to carry out specific functions. The discovery of two additional regulators of intracellular calcium further highlights how central calcium signaling is to many aspects of cell biology and how carefully the signal is controlled and regulated. Although both TMTC1 and TMTC2 appeared to disrupt calcium sequestering, only TMTC2 appeared to do so in cohort with calnexin. The precise mechanism for how TMTC1 and TMTC2 regulate SERCA2B activity is unclear, and future studies will be aimed to further investigate how TMTC1 and TMTC2 influence calcium homeostasis.

Acknowledgments—We are grateful to Dr. L. Regan (Yale University, New Haven, CT) for generously providing the in silico library of TPR proteins. We thank Dr. J. Christianson (University of Oxford, Oxford, UK) and Dr. S. Shaffer and K. Green (Proteomics and Mass Spectrometry Facility, University of Massachusetts Medical School, Worcester, MA) for their help regarding liquid chromatography-mass spectrometry/mass spectrometry experiments and analysis. We acknowledge the following members of the Hebert laboratory for fruitful discussions and critical reading of this manuscript: L. Lamriben, A Tannous, and Dr. K. Chandrasekhar.

REFERENCES

1. Voeltz, G. K., Rolls, M. M., and Rapoport, T. A. (2002) Structural organization of the endoplasmic reticulum. *EMBO Rep.* **3,** 944–950
2. Levine, T., and Rabouille, C. (2005) Endoplasmic reticulum: one continuous network compartmentalized by extrinsic cues. *Curr. Opin. Cell Biol.* **17,** 362–368
3. Carvalho, P., Goder, V., and Rapoport, T. A. (2006) Distinct ubiquitin-ligase complexes define convergent pathways for the degradation of ER proteins. *Cell* **126,** 361–373
4. Mueller, B., Klemm, E. J., Spooner, E., Claessen, J. H., and Ploegh, H. L. (2008) SEL1L nucleates a protein complex required for dislocation of misfolded glycoproteins. *Proc. Natl. Acad. Sci. U.S.A.* **105,** 12325–12330
5. Christianson, J. C., Shaler, T. A., Tyler, R. E., and Kopito, R. R. (2008) OS-9 and GRP94 deliver mutant α1-antitrypsin to the Hrd1-SEL1L ubiquitin ligase complex for ERAD. *Nat. Cell Biol.* **10,** 272–282
6. Hebert, D. N., and Molinari, M. (2007) In and out of the ER: protein folding, quality control, degradation, and related human diseases. *Physiol. Rev.* **87,** 1377–1408
7. English, A. R., Zurek, N., and Voeltz, G. K. (2009) Peripheral ER structure and function. *Curr. Opin. Cell Biol.* **21,** 596–602
8. Lynes, E. M., Raturi, A., Shenkman, M., Ortiz Sandoval, C., Yap, M. C., Wu, J., Janowicz, A., Myhill, N., Benson, M. D., Campbell, R. E., Berthiaume, L. G., Lederkremer, G. Z., and Simmen, T. (2013) Palmitoylation is the switch that assigns calnexin to quality control or ER calcium signaling. *J. Cell Sci.* **126,** 3893–3903

9. D'Andrea, L. D., and Regan, L. (2003) TPR proteins: the versatile helix. *Trends Biochem. Sci.* **28,** 655–662
10. Das, A. K., Cohen, P. W., and Barford, D. (1998) The structure of the tetratricopeptide repeats of protein phosphatase 5: implications for TPR-mediated protein-protein interactions. *EMBO J.* **17,** 1192–1199
11. Scheufler, C., Brinker, A., Bourenkov, G., Pegoraro, S., Moroder, L., Bartunik, H., Hartl, F. U., and Moarefi, I. (2000) Structure of TPR domain-peptide complexes: critical elements in the assembly of the Hsp70-Hsp90 multichaperone machine. *Cell* **101,** 199–210
12. Chang, H. C., Nathan, D. F., and Lindquist, S. (1997) *In vivo* analysis of the Hsp90 cochaperone Sti1 (p60). *Mol. Cell. Biol.* **17,** 318–325
13. Lazarus, M. B., Nam, Y., Jiang, J., Sliz, P., and Walker, S. (2011) Structure of human *O*-GlcNAc transferase and its complex with a peptide substrate. *Nature* **469,** 564–567
14. Wu, Y., and Sha, B. (2006) Crystal structure of yeast mitochondrial outer membrane translocon member Tom70p. *Nat. Struct. Mol. Biol.* **13,** 589–593
15. Rutkowski, D. T., Kang, S. W., Goodman, A. G., Garrison, J. L., Taunton, J., Katze, M. G., Kaufman, R. J., and Hegde, R. S. (2007) The role of p58IPK in protecting the stressed endoplasmic reticulum. *Mol. Biol. Cell* **18,** 3681–3691
16. Petrova, K., Oyadomari, S., Hendershot, L. M., and Ron, D. (2008) Regulated association of misfolded endoplasmic reticulum lumenal proteins with p58/DNAJc3. *EMBO J.* **27,** 2862–2872
17. UniProt Consortium (2013) Update on activities at the Universal Protein Resource (UniProt) in 2013. *Nucleic Acids Res.* **41,** D43–D47
18. Karpenahalli, M. R., Lupas, A. N., and Söding, J. (2007) TPRpred: a tool for prediction of TPR-, PPR-, and SEL1-like repeats from protein sequences. *BMC Bioinformatics* **8,** 2
19. Hessa, T., Meindl-Beinker, N. M., Bernsel, A., Kim, H., Sato, Y., Lerch-Bader, M., Nilsson, I., White, S. H., and von Heijne, G. (2007) Molecular code for transmembrane-helix recognition by the Sec61 translocon. *Nature* **450,** 1026–1030
20. Altschul, S. F., Gish, W., Miller, W., Myers, E. W., and Lipman, D. J. (1990) Basic local alignment search tool. *J. Mol. Biol.* **215,** 403–410
21. Sievers, F., Wilm, A., Dineen, D., Gibson, T. J., Karplus, K., Li, W., Lopez, R., McWilliam, H., Remmert, M., Söding, J., Thompson, J. D., and Higgins, D. G. (2011) Fast, scalable generation of high-quality protein multiple sequence alignments using Clustal Omega. *Mol. Syst. Biol.* **7,** 539
22. Svedine, S., Wang, T., Halaban, R., and Hebert, D. N. (2004) Carbohydrates act as sorting determinants in ER-associated degradation of tyrosinase. *J. Cell Sci.* **117,** 2937–2949
23. Tamura, T., Cormier, J. H., and Hebert, D. N. (2011) Characterization of early EDEM1 protein maturation events and their functional implications. *J. Biol. Chem.* **286,** 24906–24915
24. Pfaffl, M. W. (2001) A new mathematical model for relative quantification in real-time RT-PCR. *Nucleic Acids Res.* **29,** e45
25. Letunic, I., Doerks, T., and Bork, P. (2012) SMART 7: recent updates to the protein domain annotation resource. *Nucleic Acids Res.* **40,** D302–D305
26. Magliery, T. J., and Regan, L. (2005) Sequence variation in ligand binding sites in proteins. *BMC Bioinformatics* **6,** 240
27. Bendtsen, J. D., Nielsen, H., von Heijne, G., and Brunak, S. (2004) Improved prediction of signal peptides: SignalP 3.0. *J. Mol. Biol.* **340,** 783–795
28. Ota, T., Suzuki, Y., Nishikawa, T., Otsuki, T., Sugiyama, T., Irie, R., Wakamatsu, A., Hayashi, K., Sato, H., Nagai, K., Kimura, K., Makita, H., Sekine, M., Obayashi, M., Nishi, T., Shibahara, T., Tanaka, T., Ishii, S., Yamamoto, J., Saito, K., Kawai, Y., Isono, Y., Nakamura, Y., Nagahari, K., Murakami, K., Yasuda, T., Iwayanagi, T., Wagatsuma, M., Shiratori, A., Sudo, H., Hosoiri, T., Kaku, Y., Kodaira, H., Kondo, H., Sugawara, M., Takahashi, M., Kanda, K., Yokoi, T., Furuya, T., Kikkawa, E., Omura, Y., Abe, K., Kamihara, K., Katsuta, N., Sato, K., Tanikawa, M., Yamazaki, M., Ninomiya, K., Ishibashi, T., Yamashita, H., Murakawa, K., Fujimori, K., Tanai, H., Kimata, M., Watanabe, M., Hiraoka, S., Chiba, Y., Ishida, S., Ono, Y., Takiguchi, S., Watanabe, S., Yosida, M., Hotuta, T., Kusano, J., Kanehori, K., Takahashi-Fujii, A., Hara, H., Tanase, T. O., Nomura, Y., Togiya, S., Komai, F., Hara, R., Takeuchi, K., Arita, M., Imose, N., Musashino, K., Yuuki, H., Oshima, A., Sasaki, N., Aotsuka, S., Yoshikawa, Y., Matsunawa, H., Ichihara, T., Shiohata, N., Sano, S., Moriya, S., Momiyama, H., Satoh, N., Takami, S., Terashima, Y., Suzuki, O., Nakagawa, S., Senoh, A., Mizoguchi, H., Goto, Y., Shimizu, F., Wakebe, H., Hishigaki, H., Watanabe, T., Sugiyama, A., Takemoto, M., Kawakami, B., Yamazaki, M., Watanabe, K., Kumagai, A., Itakura, S., Fukuzumi, Y., Fujimori, Y., Komiyama, M., Tashiro, H., Tanigami, A., Fujiwara, T., Ono, T., Yamada, K., Fujii, Y., Ozaki, K., Hirao, M., Ohmori, Y., Kawabata, A., Hikiji, T., Kobatake, N., Inagaki, H., Ikema, Y., Okamoto, S., Okitani, R., Kawakami, T., Noguchi, S., Itoh, T., Shigeta, K., Senba, T., Matsumura, K., Nakajima, Y., Mizuno, T., Morinaga, M., Sasaki, M., Togashi, T., Oyama, M., Hata, H., Watanabe, M., Komatsu, T., Mizushima-Sugano, J., Satoh, T., Shirai, Y., Takahashi, Y., Nakagawa, K., Okumura, K., Nagase, T., Nomura, N., Kikuchi, H., Masuho, Y., Yamashita, R., Nakai, K., Yada, T., Nakamura, Y., Ohara, O., Isogai, T., and Sugano, S. (2004) Complete sequencing and characterization of 21,243 full-length human cDNAs. *Nat. Genet.* **36,** 40–45
29. Gerhard, D. S., Wagner, L., Feingold, E. A., Shenmen, C. M., Grouse, L. H., Schuler, G., Klein, S. L., Old, S., Rasooly, R., Good, P., Guyer, M., Peck, A. M., Derge, J. G., Lipman, D., Collins, F. S., Jang, W., Sherry, S., Feolo, M., Misquitta, L., Lee, E., Rotmistrovsky, K., Greenhut, S. F., Schaefer, C. F., Buetow, K., Bonner, T. I., Haussler, D., Kent, J., Kiekhaus, M., Furey, T., Brent, M., Prange, C., Schreiber, K., Shapiro, N., Bhat, N. K., Hopkins, R. F., Hsie, F., Driscoll, T., Soares, M. B., Casavant, T. L., Scheetz, T. E., Brownstein, M. J., Usdin, T. B., Toshiyuki, S., Carninci, P., Piao, Y., Dudekula, D. B., Ko, M. S., Kawakami, K., Suzuki, Y., Sugano, S., Gruber, C. E., Smith, M. R., Simmons, B., Moore, T., Waterman, R., Johnson, S. L., Ruan, Y., Wei, C. L., Mathavan, S., Gunaratne, P. H., Wu, J., Garcia, A. M., Hulyk, S. W., Fuh, E., Yuan, Y., Sneed, A., Kowis, C., Hodgson, A., Muzny, D. M., McPherson, J., Gibbs, R. A., Fahey, J., Helton, E., Ketteman, M., Madan, A., Rodrigues, S., Sanchez, A., Whiting, M., Madari, A., Young, A. C., Wetherby, K. D., Granite, S. J., Kwong, P. N., Brinkley, C. P., Pearson, R. L., Bouffard, G. G., Blakesly, R. W., Green, E. D., Dickson, M. C., Rodriguez, A. C., Grimwood, J., Schmutz, J., Myers, R. M., Butterfield, Y. S., Griffith, M., Griffith, O. L., Krzywinski, M. I., Liao, N., Morin, R., Palmquist, D., Petrescu, A. S., Skalska, U., Smailus, D. E., Stott, J. M., Schnerch, A., Schein, J. E., Jones, S. J., Holt, R. A., Baross, A., Marra, M. A., Clifton, S., Makowski, K. A., Bosak, S., Malek, J., and M. G. C. Project Team (2004) The status, quality, and expansion of the NIH full-length cDNA project: the Mammalian Gene Collection (MGC). *Genome Res.* **14,** 2121–2127
30. Sayers, E. W., Barrett, T., Benson, D. A., Bryant, S. H., Canese, K., Chetvernin, V., Church, D. M., DiCuccio, M., Edgar, R., Federhen, S., Feolo, M., Geer, L. Y., Helmberg, W., Kapustin, Y., Landsman, D., Lipman, D. J., Madden, T. L., Maglott, D. R., Miller, V., Mizrachi, I., Ostell, J., Pruitt, K. D., Schuler, G. D., Sequeira, E., Sherry, S. T., Shumway, M., Sirotkin, K., Souvorov, A., Starchenko, G., Tatusova, T. A., Wagner, L., Yaschenko, E., and Ye, J. (2009) Database resources of the National Center for Biotechnology Information. *Nucleic Acids Res.* **37,** D5–D15
31. Walter, P., and Ron, D. (2011) The unfolded protein response: from stress pathway to homeostatic regulation. *Science* **334,** 1081–1086
32. Mostov, K. E., DeFoor, P., Fleischer, S., and Blobel, G. (1981) Co-translational membrane integration of calcium pump protein without signal sequence cleavage. *Nature* **292,** 87–88
33. Giorda, K. M., Raghava, S., and Hebert, D. N. (2012) The simian virus 40 late viral protein VP4 disrupts the nuclear envelope for viral release. *J. Virol.* **86,** 3180–3192
34. Pearse, B. R., and Hebert, D. N. (2010) Lectin chaperones help direct the maturation of glycoproteins in the endoplasmic reticulum. *Biochim. Biophys. Acta* **1803,** 684–693
35. Luo, D., Broad, L. M., Bird, G. S., and Putney, J. W., Jr. (2001) Signaling pathways underlying muscarinic receptor-induced $[Ca^{2+}]_i$ oscillations in HEK293 cells. *J. Biol. Chem.* **276,** 5613–5621
36. Wu, X., Babnigg, G., Zagranichnaya, T., and Villereal, M. L. (2002) The role of endogenous human Trp4 in regulating carbachol-induced calcium oscillations in HEK-293 cells. *J. Biol. Chem.* **277,** 13597–13608
37. Brini, M., and Carafoli, E. (2009) Calcium pumps in health and disease. *Physiol. Rev.* **89,** 1341–1378
38. Wu, C., Macleod, I., and Su, A. I. (2013) BioGPS and MyGene.info: organizing online, gene-centric information. *Nucleic Acids Res.* **41,** D561–D565

39. Nilsson, I. M., and von Heijne, G. (1993) Determination of the distance between the oligosaccharyltransferase active site and the endoplasmic reticulum membrane. *J. Biol. Chem.* **268,** 5798–5801
40. Zeytuni, N., and Zarivach, R. (2012) Structural and functional discussion of the tetra-trico-peptide repeat, a protein interaction module. *Structure* **20,** 397–405
41. Swanton, E., High, S., and Woodman, P. (2003) Role of calnexin in the glycan-independent quality control of proteolipid protein. *EMBO J.* **22,** 2948–2958
42. Roderick, H. L., Lechleiter, J. D., and Camacho, P. (2000) Cytosolic phosphorylation of calnexin controls intracellular Ca^{2+} oscillations via an interaction with SERCA2b. *J. Cell Biol.* **149,** 1235–1248
43. Simpson, J. C., Joggerst, B., Laketa, V., Verissimo, F., Cetin, C., Erfle, H., Bexiga, M. G., Singan, V. R., Hériché, J. K., Neumann, B., Mateos, A., Blake, J., Bechtel, S., Benes, V., Wiemann, S., Ellenberg, J., and Pepperkok, R. (2012) Genome-wide RNAi screening identifies human proteins with a regulatory function in the early secretory pathway. *Nat Cell Biol.* **14,** 764–774
44. Landry, J. J., Pyl, P. T., Rausch, T., Zichner, T., Tekkedil, M. M., Stütz, A. M., Jauch, A., Aiyar, R. S., Pau, G., Delhomme, N., Gagneur, J., Korbel, J. O., Huber, W., and Steinmetz, L. M. (2013) The genomic and transcriptomic landscape of a HeLa cell line. *G3* **3,** 1213–1224